

Light-shift mitigation in a microcell-based atomic clock with Symmetric Auto-Balanced Ramsey spectroscopy

M. Abdel Hafiz,¹ C. Carlé,¹ N. Passilly,¹ J. M. Danet,² C. E. Calosso,³ and R. Boudot¹

¹*FEMTO-ST, CNRS, Université Bourgogne Franche-Comté, Besançon, France*

²*Syrlinks, 28 rue Robert Keller, Cesson-Sevigne, France*

³*INRIM, Strada delle Cacce 91, Torino, Italy*

(*Electronic mail: moustafa.abdel@femto-st.fr)

The mid-term fractional frequency stability of miniaturized atomic clocks can be limited by light-shift effects. In this Letter, we demonstrate the implementation of a symmetric Auto-Balanced Ramsey (SABR) interrogation sequence in a microcell-based atomic clock based on coherent population trapping (CPT). Using this advanced protocol, the sensitivity of the clock frequency to laser power, microwave power and laser frequency variations is reduced, at least by one order of magnitude, in comparison with continuous-wave (CW) or Ramsey interrogation schemes. Light-shift mitigation obtained with the SABR sequence benefits greatly to the clock Allan deviation for integration times between 10^2 and 10^5 s. These results demonstrate that such interrogation techniques are of interest to enhance timekeeping performances of chip-scale atomic clocks.

The development of low-SWaP (size-weight-power) frequency references with enhanced frequency stability is of crucial importance in a wide range of applications including timing, navigation, positioning, security, communication or scientific systems¹. In these domains, microwave chip-scale atomic clocks (CSACs)²⁻⁶ based on coherent population trapping (CPT) have met a remarkable success by offering a daily drift about 100 times smaller than commonly-used oven-controlled quartz oscillators.

Light-shifts are known to be an important contribution to the fractional frequency stability of miniaturized atomic clocks for integration times higher than 100 s. Multiple approaches have then been proposed to mitigate their detrimental impact. Some efforts were oriented towards the extraction of the actual laser or cell temperature, from the atomic response itself, in order to reduce the negative impact of temperature gradients between these key components and their respective temperature sensors^{2,5,7}. Other sophisticated methods include the active stabilization of a specific laser microwave modulation index that reduces laser power-induced frequency instabilities^{3,5,8-10}, possibly combined with the compensation for the laser aging⁶, or the implementation of advanced tailored interrogation sequences using laser power modulation¹¹. Deposition of gold micro-discs, used as privileged alkali condensation spots onto the cell windows was also shown to avoid the progressive obstruction of the transmitted laser light¹². An alternative and straightforward approach to mitigate light-shifts in CPT clocks is to probe the clock transition with Ramsey spectroscopy^{13,14}. Mainly investigated in compact vapor cell clocks¹⁵, Ramsey-CPT spectroscopy has recently stimulated some research interest in miniaturized atomic clocks. The generation of robust Ramsey-CPT sequences with directly-modulated lasers was demonstrated in Refs^{16,17}, while the spectroscopy, clock operation and evidence of light-shift mitigation was reported with Ramsey-CPT in buffer-gas filled microfabricated vapor cells^{18,19}.

Nevertheless, Ramsey-CPT spectroscopy suffers from a residual sensitivity to light-shifts, experienced by the atoms during the light pulses. Advanced Ramsey-based tailored interrogation protocols, based on two consecutive Ramsey sequences with different dark times, have then been proposed and demonstrated in various types of atomic clocks for enhanced light-shift mitigation²⁰⁻²⁶. In standard vapor cell clocks, it was demonstrated that the symmetry of the interrogation was of crucial importance to tackle an atomic memory effect, mainly linked to the limited duty cycle of the probing sequence, and then to optimize light-shift mitigation^{11,22}. While these techniques have shown outstanding efficiency, they have not yet been explored in microfabricated cells, as those employed in CSACs.

In microcells, the shorter timescales of the light pulse sequence, imposed by the reduced CPT coherence lifetime, raises the question of a possible amplification of the atomic memory effect. In addition, the loss of resolution in the light-shift measurement, as the difference between the applied dark times is decreased, deserves specific attention to ensure that enough precision is kept to provide improved clock frequency stability.

In this letter, we study and demonstrate the implementation of a symmetric Auto-Balanced Ramsey (SABR) sequence in a CPT-based microcell atomic clock. For sake of simplicity and proof-of-concept demonstration, the pulsed optical sequence is applied with an external acousto-optical modulator (AOM). In comparison with the standard Rabi or Ramsey-CPT interrogation schemes, we demonstrate that the SABR method reduces the sensitivity of the clock frequency to laser power, microwave power and laser frequency variations, by a factor higher than 10. Furthermore, we strengthen the importance of the sequence symmetry and its ability to annihilate the consequences of the atomic memory effect in mm-scale cells. We also show that the use of SABR improves the clock Allan deviation for integration times between 10^2 and 10^5 s, especially by reducing the impact of temperature-induced light-shift effects.

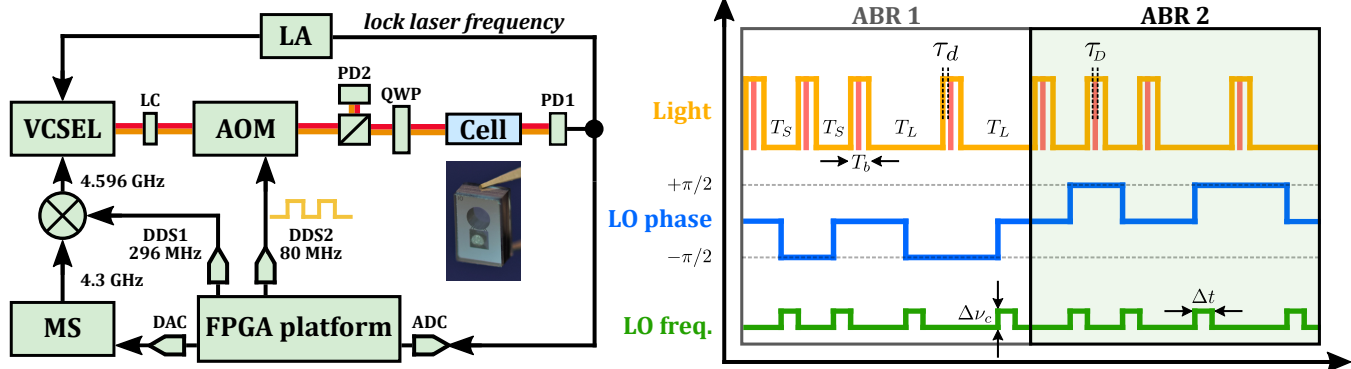


FIG. 1. (Color online) Left: CPT clock setup and basic architecture of a SABR sequence. LC: collimation lens, QWP: quarter-wave plate, LA: lock-in amplifier, ADC: analog-to-digital converter, DAC: digital-to-analog converter, MS: microwave synthesizer. Right: simplified scheme for the SABR sequence.

Figure 1 presents the CPT clock experimental setup. The heart of the clock is a pill-dispenser microfabricated Cs vapor cell^{27,28} filled with about 90 Torr of Neon. The cell is temperature-stabilized at 70°C. A static magnetic field of 10 μ T is applied to raise the Zeeman degeneracy and isolate the 0-0 clock transition. Atoms in the cell interact with a dual-frequency optical field produced by direct microwave modulation of a vertical-cavity surface emitting laser (VCSEL)²⁹, tuned on the Cs D₁ line, and such that both first-order optical sidebands induce the CPT resonance. Except when willingly varied for tests, the microwave power that enters the VCSEL is about -2.3 dBm. At the output of the laser, an AOM, driven by a switchable radiofrequency (RF) signal, is used to generate the pulsed optical sequence. Tuning the power of the RF signal permits control of the total laser power incident onto the cell. The 0.5-mm diameter laser beam is then sent through the Cs vapor microcell and detected at its output with a photodiode.

For this study, we have used a field-programmable gate array (FPGA)-based digital control electronics platform³⁰. The latter allows fast computation and feedback to the experiment, such that the generated sequence is readjusted every clock cycle. In this ecosystem, the output 4.596 GHz signal that drives the VCSEL is obtained by mixing a 4.3 GHz from a synthesizer and a 296 MHz signal generated by a direct digital synthesizer (DDS1). A second DDS (DDS2) delivers the 80 MHz RF signal that drives the AOM. This signal can be turned on and off with the help of embedded RF switches. All DDS are clocked with an ultra-pure 860 MHz signal obtained by frequency division by 5 of the synthesizer 4.3 GHz signal. The absolute phase noise of the output 4.596 GHz was measured to be -118 dBc/Hz at an offset frequency $f = 1$ kHz. This phase noise reduces the Dick effect contribution³¹ to a negligible level for such a microcell-based clock. The microwave source is referenced to an active hydrogen maser. In the following, the optically-carried 9.192 GHz signal of frequency ν_{LO} , used to probe the atomic transition, is named as the

local oscillator (LO) signal. In clock operation, the value of ν_{LO} is changed by digitally changing the output frequency of DDS1. Corrections applied to DDS1 are then recorded and used as frequency data for analysis. The tested SABR sequence, shown in Fig. 1, is similar to the one described in Ref.²². It consists of two consecutive ABR sequences (ABR 1 and ABR 2). Each ABR sequence consists in turn of four consecutive Ramsey-CPT sequences with light pulses of length T_b . The two first Ramsey-CPT patterns use a short dark time T_S while the two following ones use a long dark time T_L . A $\pm\pi/2$ phase jump is applied onto the optically-carried microwave interrogating signal during the dark times by acting on DDS1, in order to successively measure the transmitted signals on respective sides of the central fringe. This yields the extraction of error signals, noted ε_S (for the short dark time pattern) and ε_L (for the long dark time pattern). In the second ABR sequence (ABR 2), the light pulse pattern is identical while the LO phase modulation pattern is the mirror symmetric to the one used in the first ABR sequence (ABR 1). In vapor cell experiments, the use of a symmetric ABR sequence is of crucial importance to cancel a memory effect of the atoms and then to improve the efficiency of the light-shift rejection²². Ultimately, two error signals are calculated, ensuring that information is extracted at all pulses for both correction signals and then preventing the negative impact of aliasing on the short-term stability²². The error signal $\varepsilon_+ = \varepsilon_S + \varepsilon_L$ is used to correct the LO frequency. The error signal $\varepsilon_- = \varepsilon_S - \varepsilon_L$ is extracted to correct the value of an additional phase jump φ_c , applied during dark times, that compensates for the light-induced phase shift built up during the previous light pulse. The phase jump φ_c is obtained by changing the LO frequency by the amount $\Delta\nu_c$ for a time Δt .

In all the tests reported in this manuscript, the pulses length T_b is set to 183 μ s and the atomic signal is sampled after a delay τ_d of 33 μ s, to account for the delay induced by the anti-aliasing filter. The latter,

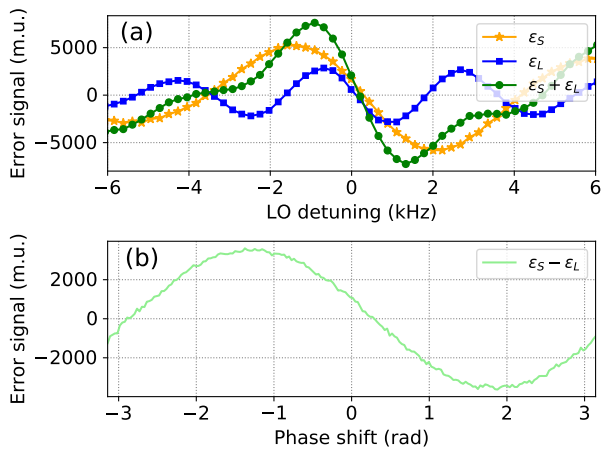


FIG. 2. (Color online) (a) Error signals ϵ_S , ϵ_L , ϵ_+ as a function of the LO detuning from the value of 9 192 682 200 Hz, and (b) Error signal ϵ_- as a function of the phase jump φ_c during the dark time, extracted from a SABR sequence.

a 25.6 kHz low-pass filter, averages the photodiode voltage over about 20 μs and is responsible of the actual duration τ_D of the detection window.

Figure 2(a) shows error signals ϵ_S , ϵ_L , and ϵ_+ extracted from a SABR sequence performed on the Cs-Ne microcell. It is clear that the initial error signal ϵ_S , extracted from the sequence with the shortest dark time T_S , is higher in amplitude and broader than the error signal ϵ_L obtained for the longest sequence. Their zero-crossings, mainly shifted from the natural Cs atom frequency because of the buffer-gas induced collisional shift, do not coincide due to the variation of the light-shift magnitude with the dark time value. The error signal $\epsilon_+ = \epsilon_S + \epsilon_L$ benefits from a higher amplitude, that justifies its use for stabilization of the LO frequency. The error signal $\epsilon_- = \epsilon_S - \epsilon_L$, plotted in Fig. 2(b) versus the phase jump φ_c applied during the dark time, exhibits in open-loop configuration a zero-crossing point at a non-null value of φ_c (~ 0.3 rad), where the light-shift is compensated in closed loop.

Figure 3(a) shows the dependence of the clock frequency to laser power variations, in the standard CW regime, the Ramsey-CPT case, the SABR case and the non-symmetric ABR case, respectively. In the Ramsey-CPT case, the light-shift coefficient is 0.79 Hz/ μW . In the SABR case, the latter is reduced by a factor 26 to 0.03 Hz/ μW . This coefficient is 470 times smaller than the one measured in the standard CW scheme (14 Hz/ μW). We have also performed the same measurement when the ABR clock sequence is reduced to the first part (ABR 1). In this non-symmetric case, the memory effect is responsible for a shift of the clock frequency by more than 250 Hz. Without symmetry, the ABR protocol does not give any significant advantage and even leads to a slight deterioration, with respect

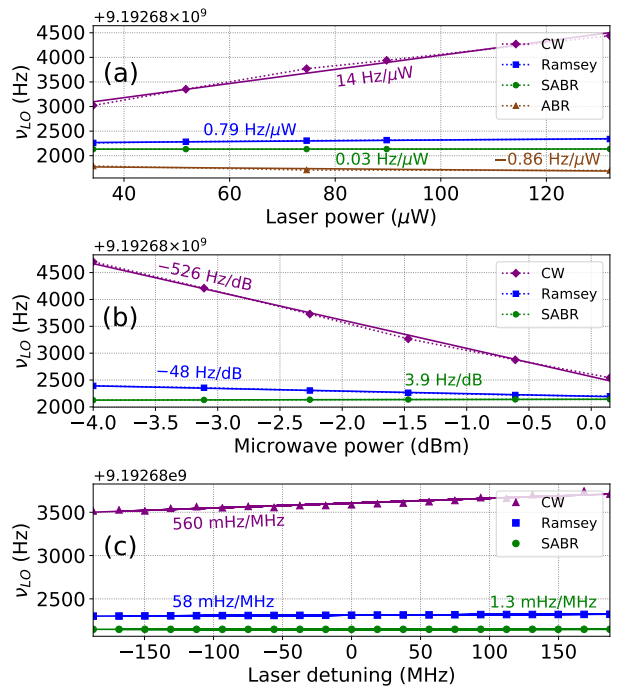


FIG. 3. (Color online) Clock frequency versus (a) the laser power, (b) the microwave power or (c) the laser carrier frequency, in the standard CW regime, the Ramsey-CPT case, the SABR case or the ABR case. Experimental data are fitted by linear functions, shown as solid lines, from which a linear light-shift coefficient is extracted.

to the Ramsey-CPT case in microcells. This result attests that the memory effect is strong in microcells, highlighting the importance of the sequence symmetry. Variations of the microwave power that drives the VCSEL can also induce significant shifts of the CPT clock frequency^{3,8,9}. We have then measured this sensitivity with the SABR sequence. Corresponding results are shown on Fig. 3(b), in comparison with those obtained with the CW or Ramsey-CPT schemes. In the SABR case, a sensitivity of +3.9 Hz/dB is measured, to be compared with a slope of -48 Hz/dB and -526 Hz/dB in the Ramsey-CPT and CW cases, respectively. Figure 3(c) depicts an additional sensitivity measurement with the laser frequency. Calibration of the laser frequency change was performed using absorption profiles detected at the cell output. Here again, we observe a strong reduction of the light-shift coefficient, reduced from 58 mHz/MHz in the Ramsey-CPT case and even 560 mHz/MHz in CW regime down to 1.3 mHz/MHz in the SABR case.

Finally, frequency stability measurements of the microcell CPT clock operating with Ramsey-CPT or SABR-CPT sequences have been performed. These tests were conducted on the same setup, with quasi-identical environment conditions. The total laser power at the cell input is about 72 μW . Allan deviations are shown in Fig. 4.

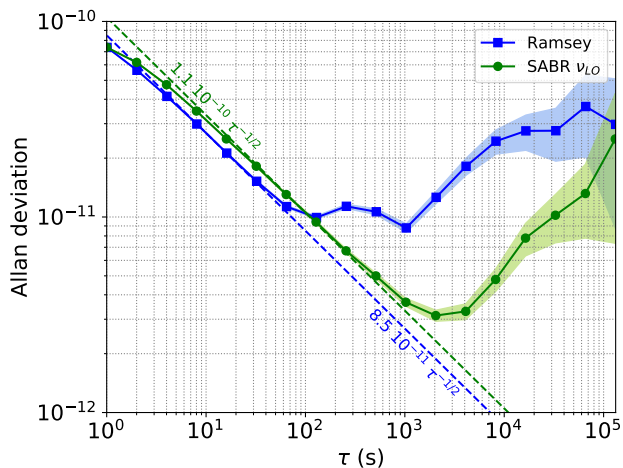


FIG. 4. (Color online) Allan deviation of the clock frequency in Ramsey-CPT and SABR-CPT regimes.

In the Ramsey-CPT case, the clock short-term stability is about $8.5 \times 10^{-11} \tau^{-1/2}$ until 60 s. We identified that the "bump" between 60 and 10^3 s was attributed to temperature fluctuations of the laboratory. For $\tau > 10^3$ s, a degradation is observed, yielding the level of 3×10^{-11} at 10^5 s.

In the SABR case, the clock short-term stability is slightly degraded, with the level of 1.1×10^{-10} at 1 s. At the opposite, the clock performance is clearly improved in the 10^2 - 10^5 s range. We observed with SABR a significant suppression of the correlation of the clock frequency with temperature variations of the laboratory, benefiting greatly to the clock Allan deviation that averages down until 2000 s, at the level of 3×10^{-12} . It is also interesting to note that, with SABR, a correlation was observed between the lab temperature and the routinely measured phase jump φ_c . These results confirm further that the SABR method efficiently mitigates light-shifts in microcells and improves the mid-term stability of miniaturized clocks, without any significant deterioration of the short-term stability.

For $\tau > 3000$ s, the Allan deviation remains degraded, reaching the level of about 2.5×10^{-11} at 10^5 s. However, several arguments tend to exonerate light-shift effects. From Fig. 3, we calculate that this stability level should be explained by fluctuations at 1 day of laser power and laser frequency, such that $\Delta P = 7.6 \mu\text{W}$ ($\Delta P/P = 10.6\%$), and $\Delta f = 177$ MHz ($\Delta f/f = 5.2 \times 10^{-7}$), respectively. These values are high in comparison with those reported in the literature^{3,28,32}. Variations $\Delta P_{\mu\text{W}}$ of the microwave power of only 0.06 dB at 1 day might be more suspected^{3,6,28} to justify the stability limitation. However, this assumption is counterbalanced by two observations. First, Allan deviation results obtained at 1 day are comparable for SABR and Ramsey-CPT cases whereas light-shift coefficients in the Ramsey case are at least one order of magnitude higher. Second, in both Ramsey and SABR cases, we observed

that the clock frequency constantly drifted with a negative slope. This similar frequency drift sign, observed in both regimes, is contradictory with the fact that light-shift coefficients reported in Fig. 3(b), obtained in Ramsey and SABR cases, exhibit opposite signs. We have also checked that the temperature dependence of the buffer gas collisional shift^{33,34}, the Zeeman shift, barometric effects³⁵ or alkali condensation on the cell windows¹² could not explain the measured stability level at 1 day. To date, the clock stability limitation at 1 day on this setup is suspected to come from a possible unstable cell inner atmosphere. This could be related to Ne buffer gas permeation through the glass windows³⁶, materials degassing, or dispenser pollution³⁷.

In conclusion, we have explored the implementation of Auto-Balanced Ramsey (ABR) spectroscopy, for light-shift mitigation, in a microcell-based atomic clock. Despite the use of patterns with optical pulses and dark time durations of only a few hundreds of microseconds, this technique, provided that symmetry of the pattern is well applied, reduces the dependence of the clock frequency to laser field parameters variations by more than two orders of magnitude, with respect to the standard CW-regime approach, commonly used in commercial CSACs. We also demonstrated that SABR contributes to improve the clock Allan deviation of a microcell CPT clock between 10^2 and 10^5 s, where light-shifts are predominant.

This work was partly funded by the Délégation Générale de l'Armement (DGA), Centre National des Etudes Spatiales (CNES), Agence Innovation Défense (AID), Conseil Régional Bourgogne Franche-Comté with the HACES project (grant 2018-04768), and in part by Agence Nationale de la Recherche (ANR) in the frame of the LabeX FIRST-TF (Grant ANR 10-LABX-48-01), EquipX Oscillator-IMP (Grant ANR 11-EQPX-0033), ASTRID PULSACION (Grant ANR-19-ASTR-0013-01) projects and EIPHI Graduate school (Grant ANR-17-EURE-0002). This work was partly supported by the french RENATECH network and FEMTO-ST technological facility (MIMENTO). The authors thank deeply J. P. McGilligan (Strathclyde University) for careful reading of the manuscript.

DATA AVAILABILITY STATEMENT

The data supporting the findings of this study are available from the corresponding author upon reasonable request.

¹J. Kitching, Chip-scale atomic devices, *Appl. Phys. Rev.* **5**, 031302 (2018).

²R. Lutwak, A. Rahsed, M. Varghese, G. Tepolt, J. LeBlanc, M. Mescher, D. K. Serkland, K. M. Geib, G. M. Peake and S. Romisch, The Chip-Scale Atomic Clock-Prototype Evaluation,

- Proceedings of the 39th Annual Precise Time and Time Interval Meeting, pp. 269–290 (2007).
- ³Y. Zhang, W. Yang, S. Zhang and J. Zhao, Rubidium chip-scale atomic clock with improved long-term stability through light intensity optimization and compensation for laser frequency detuning, *J. Opt. Soc. Am. B* **33**, 8, 1756 (2016).
 - ⁴H. Zhang, H. Hans, N. Tharayil, A. Shirane, M. Suzuki, K. Harasaka, K. Adachi, S. Goka, S. Yanagimachi and K. Okada, UL-PAC: A miniaturized ultra-low power atomic clock, *IEEE Journ. Solid State Circuits* **54**, 11, 3135–3148 (2019).
 - ⁵R. Vicarini, M. Abdel Hafiz, V. Maurice, N. Passilly, E. Kroemer, L. Ribetto, V. Gaff, C. Gorecki, S. Galliou and R. Boudot, Mitigation of temperature-induced light-shift effects in miniaturized atomic clocks, *IEEE Trans. Ultrason. Ferroelec. Freq. Contr.* **66**, 12, 1962–1967 (2019).
 - ⁶S. Yanagimachi, K. Harasaka, R. Suzuki, M. Suzuki and S. Goka, Reducing frequency drift caused by light shift in coherent population trapping-based low-power atomic clocks, *Appl. Phys. Lett.* **116**, 104102 (2020).
 - ⁷V. Shah, V. Gerginov, P. D. D. Schwindt, S. Knappe, L. Hollberg, and J. Kitching, Continuous light-shift correction in modulated coherent population trapping clocks, *Opt. Lett.* **31**, 1851–1853 (2006).
 - ⁸M. Zhu and L. S. Cutler, U.S. Patent 6,201,821 (2001).
 - ⁹V. Shah, V. Gerginov, P. D. D. Schwindt, S. Knappe, L. Hollberg, and J. Kitching, Continuous light-shift correction in modulated coherent population trapping clocks, *Appl. Phys. Lett.* **89**, 151124 (2006).
 - ¹⁰B. H. McGuyer, Y. Y. Jau and W. Happer, Simple method of light-shift suppression in optical pumping systems, *Appl. Phys. Lett.* **94**, 251110 (2009).
 - ¹¹M. Abdel Hafiz, R. Vicarini, N. Passilly, C. E. Calosso, V. Maurice, J. W. Pollock, A. V. Taichenachev, V. I. Yudin, J. Kitching and R. Boudot, Protocol for light-shift compensation in a continuous-wave microcell atomic clock, *Phys. Rev. Appl.* **14**, 034015 (2020).
 - ¹²S. Karlen, T. Overstolz, J. Gobet, J. Haesler, F. Droz and S. Lecomte, Gold microdiscs as alkali preferential condensation spots for cell clock long-term frequency improvement, *Proc. European Frequency and Time Forum 2018*, Torino, Italy (2018). DOI: 10.1109/EFTF.2018.8409005
 - ¹³T. Zanon, S. Guérandel, E. de Clercq, D. Holleville, N. Dimarcq and A. Clairon, High Contrast Ramsey Fringes with Coherent-Population-Trapping Pulses in a Double Lambda Atomic System, *Phys. Rev. Lett.* **94**, 193002 (2005).
 - ¹⁴N. Castagna, R. Boudot, S. Guérandel, E. de Clercq, N. Dimarcq and A. Clairon Investigations on continuous and pulsed interrogation for a CPT atomic clock, *IEEE Trans. Ultrason. Ferroelec. Freq. Contr.* **56**, 2, 246–253 (2009).
 - ¹⁵M. Abdel Hafiz, G. Coget, P. Yun, S. Guérandel, E. de Clercq and R. Boudot, A high-performance Raman-Ramsey Cs vapor cell atomic clock, *J. Appl. Phys.* **121**, 104903 (2017).
 - ¹⁶Y. Yano, S. Goka, and M. Kajita, Two-step pulse observation for Raman–Ramsey coherent population trapping atomic clocks, *Appl. Phys. Exp.* **8**, 012108 (2015).
 - ¹⁷M. Fukuoka, D. Haraguchi, and S. Goka, Light shift characteristics of Ramsey-coherent population trapping resonances excited by two-step drive current, in *Proc. Int. Freq. Control Symp., Eur. Freq. Time Forum Joint Meeting*, Orlando, FL, USA, 2019, pp. 269–290.
 - ¹⁸R. Boudot, V. Maurice, C. Gorecki and E. de Clercq, Pulsed coherent population trapping spectroscopy in microfabricated Cs–Ne vapor cells, *J. Opt. Soc. Am. B* **35**, 5, 1004–1010 (2018).
 - ¹⁹C. Carlé, M. Petersen, N. Passilly, M. Abdel Hafiz, E. de Clercq and R. Boudot, Exploring the use of Ramsey-CPT spectroscopy for a microcell-based atomic clock, *IEEE Trans. Ultrason. Ferroelec. Freq. Contr.* **68**, 10, 3249–3256 (2021).
 - ²⁰C. Sanner, N. Huntemann, R. Lange, C. Tann and E. Peik, Auto-balanced Ramsey spectroscopy, *Phys. Rev. Lett.* **120**, 053602 (2018).
 - ²¹V. Yudin, A. V. Taichenachev, M. Yu. Basalaev, T. Zanon-Willette, J. W. Pollock, M. Shuker, E. A. Donley, and J. Kitching, Generalized autobalanced Ramsey spectroscopy of clock transitions, *Phys. Rev. Appl.* **9**, 054034 (2018).
 - ²²M. Abdel Hafiz, G. Coget, M. Petersen, C. E. Calosso, S. Guérandel, E. de Clercq and R. Boudot, Symmetric autobalanced Ramsey interrogation for high-performance coherent population-trapping vapor-cell atomic clock, *Appl. Phys. Lett.* **112**, 244102 (2018).
 - ²³M. Shuker, J. W. Pollock, R. Boudot, V. I. Yudin, A. V. Taichenachev, J. Kitching and E. A. Donley, Ramsey spectroscopy with displaced frequency jumps, *Phys. Rev. Lett.* **122**, 113601 (2019).
 - ²⁴M. Shuker, J. W. Pollock, R. Boudot, V. I. Yudin, A. V. Taichenachev, J. Kitching and E. A. Donley, Reduction of light shifts in Ramsey spectroscopy with a combined error signal, *Appl. Phys. Lett.* **114**, 141106 (2019).
 - ²⁵C. Calosso, M. Gozzelino, H. Lin, F. Levi, A. Godone, S. Micalizio, Novel Techniques for Locking the Laser Frequency to the Clock Cell in Vapor Cell Standards, *Proc. 2019 Intern. Freq. Contr. Symp., Paper WeBT2.1*, Orlando, USA (2019).
 - ²⁶M. Y. Basalaev, V. I. Yudin, D. V. Kovalenko, T. Zanon-Willette, and A. V. Taichenachev, Generalized-Ramsey methods in the spectroscopy of coherent-population-trapping resonances, *Phys. Rev. A* **102**, 013511 (2020).
 - ²⁷M. Hasegawa, R. K. Chutani, C. Gorecki, R. Boudot, P. Dziuban, V. Giordano, S. Clatot, and L. Mauri, Microfabrication of cesium vapor cells with buffer gas for MEMS atomic clocks, *Sens. Actuators A* **167**, 594–601 (2011).
 - ²⁸R. Vicarini, V. Maurice, M. Abdel Hafiz, J. Rutkowski, C. Gorecki, N. Passilly, L. Ribetto, V. Gaff, V. Volant, S. Galliou, R. Boudot, Demonstration of the mass-producible feature of a Cs vapor microcell technology for miniature atomic clocks, *Sens. Actuators A* **280**, 99–106 (2018).
 - ²⁹E. Kroemer, J. Rutkowski, V. Maurice, R. Vicarini, M. Abdel Hafiz, C. Gorecki and R. Boudot, Characterization of commercially vertical-cavity surface-emitting lasers tuned on Cs D₁ line at 894.6 nm for atomic clocks, *Appl. Opt.* **55**, 31, 8839–8847 (2016).
 - ³⁰<https://m-labs.hk/experiment-control/sinara-core/>
 - ³¹J. M. Danet, M. Lours, S. Guérandel, E. de Clercq, Dick effect in a pulsed atomic clock Using coherent population trapping, *IEEE Trans. Ultrason. Ferroelec. Freq. Contr.* **61**, 4, 567–574 (2014).
 - ³²F. Gruet, F. Vecchio, C. Affolderbach, F. Pétremand, N. F. de Rooij, T. Maeder and G. Mileti, A miniature frequency stabilized VCSEL system emitting at 795 nm based on LTCC modules, *Opt. Lasers Eng.* **51**, 8, 1023–1027 (2013).
 - ³³D. Mileti, P. Dziuban, R. Boudot, M. Hasegawa, R. K. Chutani, G. Mileti, V. Giordano and C. Gorecki, Quadratic dependence on temperature of Cs 0-0 hyperfine resonance frequency in single Ne buffer gas microfabricated vapour cell, *Elec. Lett.* **46**, 15, 1069–1071 (2010).
 - ³⁴O. Kozlova, S. Guérandel and E. de Clercq, Temperature and pressure shift of the Cs clock transition in the presence of buffer gases: Ne, N₂, Ar, *Phys. Rev. A* **83**, 062714 (2011).
 - ³⁵W. Moreno, M. Pellaton, C. Affolderbach and G. Mileti, Barometric effect in vapor cell atomic clocks, *IEEE Trans. Ultrason. Ferroelec. Freq. Contr.* **65**, 8, 1500–1503 (2018).
 - ³⁶S. Abdullah, C. Affolderbach, F. Gruet and G. Mileti, Aging studies on micro-fabricated alkali buffer-gas cells for miniature atomic clocks, *Appl. Phys. Lett.* **106**, 163505 (2015).
 - ³⁷R. N. Kohn Jr, M. S. Bigelow, M. Spanjers, B. K. Stuhl, B. L. Kasch, S. E. Olson, E. A. Imhof, D. A. Hostutler, M. B. Squires, Clean, robust alkali sources by intercalation within highly oriented pyrolytic graphite, *Rev. Sci. Instr.* **91**, 035108 (2020).